Contribution from the Department of Chemistry,
University of Victoria, Victoria, BC V8W 2Y2, Canada

Bis(1,4,7-triazacyclononane)palladium(III): Characterization and Reactions of an Unusually Stable Monomeric Palladium(III) Ion

A. McAuley* and T. W. Whitcombe

Received December 4, 1987

The synthesis of the monomeric palladium(III) ion $[Pd([9]aneN_3)_2]^{3+}$ ([9]aneN$_3$: 1,4,7-triazacyclononane) as the hexafluorophosphate salt is described. Solutions of this ion exhibit exceptional kinetic stability in aqueous media as shown by the ESR spectrum of the d^7 ion. With $Pd^{II}([9]aneN_3)_2^{2+}$, electrochemical oxidation yields two one-electron cyclic voltammograms associated with oxidation to the Pd(III) and Pd(IV) states. Electrode potentials are pH dependent owing to protonation (producing $Pd(HL)(L)^{n+}$ and $Pd(HL)_2^{m+}$ (n = 3, 4; m = 4, 5)) of one or both of the ligands at an uncoordinated nitrogen site. For the nonprotonated couples, $E°(Pd([9]aneN_3)_2^{3+/2+}) = 0.37_0$ V (vs NHE) in ClO_4^- or NO_3^- media and is about 30 mV higher in acetate media. For the corresponding $Pd([9]aneN_3)_2^{4+/3+}$ couple, $E° = 0.64_0$ V (vs NHE). A detailed analysis of the pH dependences is provided. An isotropic ESR signal, g_{iso} = 2.077 (77 K) (g_{iso} = 2.08 (298 K)) is observed at low ionic strength. However, in saturated Li_2SO_4, a pseudoaxial spectrum is derived, $g_\perp$ = 2.115 and $g_\parallel$ = 2.007 (A = 26.2 G), owing to ion-pair formation. Stopped-flow kinetic experiments have been carried out with both $Pd([9]aneN_3)_2^{3+}$ and $Pd([9]aneN_3)_2^{2+}$ as reagents. Rates of reduction of the Pd(III) ion with $Co([9]aneN_3)_2^{2+}$ and Co(sepulchrate)$^{2+}$ and rates of oxidation of the Pd(II) ion with $Ni([9]aneN_3)_2^{3+}$ and $Ni(Me[9]aneN_3)_2^{3+}$, when analyzed by using a Marcus cross-correlation, led to a value of $(2 \pm 1) \times 10^{-6}$ M^{-1} s^{-1} for the $Pd([9]aneN_3)_2^{3+/2+}$ couple. The origin of this exceptionally low rate lies in the inner-sphere reorganization required to provide axial interaction of the noncoordinated nitrogens with the normally square-planar d^8 Pd(II) ion. This rate constant is contrasted with that of $(7 \pm 3) \times 10^2$ M^{-1} s^{-1} for the $Pd([9]aneN_3)_2^{4+/3+}$ couple where both reagents are octahedral in configuration. The data are compared to other d^7/d^6 exchanges, and the steric role of the ligand in the electron-transfer process is described.

Introduction

The macrocyclic ligand 1,4,7-triazacyclononane ([9]aneN$_3$; Figure 1a) has received attention recently owing to its ability to form stable complexes with a variety of first-row transition-metal ions (Ni,[1] Co,[2] Fe[3]) and with some second- and third-row elements (Ru,[4] Pt[5]). The ligand, like many nitrogen macrocyclic species, stabilizes unusual oxidation states, such as Ni(III).[1c,1d] The small size of the ring induces facial disposition onto an octahedral structure; hence, all of the simple complexes involving first-row elements exhibit an MN_6 geometry.

However, the elements of the second and third transition series are not always predisposed toward an octahedral geometry as a result of an increased crystal field stabilization energy. For Pt(II), the d^8 configuration exhibits almost exclusively a square-planar geometry.[6] This has been observed[5] in the corresponding $Pt([9]aneN_3)_2^{2+}$ complex, which may be oxidized by molecular oxygen to the Pt(IV) species where the anticipated octahedral coordination is observed. The steric demands of the ligand facilitate the oxidation of the metal center. The stability of the Pt(IV) ion has permitted its isolation and characterization.

Ligand effects also determine the oxidation behavior in a number of silver macrocyclic complexes.[7] In Ag(cyclam),$^{n+}$ coordination of the ligand generates a thermodynamic disproportionation of the Ag(I) ion to give the Ag(II) ion and silver metal.

We have recently reported[8] the synthesis and characterization of the complex $Pd([9]aneN_3)_2^{3+}$ from the corresponding Pd(II) species. This molecular ion may be considered as another example of a system where ligand disposition facilitates oxidation of the metal center. The crystal structure of the Pd(II) complex[9] has the ligand coordinated in a bidentate, square-planar manner and is isomorphous with the Pt(II) ion.[5] However, there appears to be some steric strain in the molecule. The presence of the available axial lone pairs on the noncoordinated nitrogen atoms perturbs the orbital energy levels and permits the formation of a Pd(III) structure (Figure 1), which has a strain-free octahedral geometry. In contrast to platinum, both 1e oxidations [Pd(II) → Pd(III) → Pd(IV)] may be examined electrochemically. The occurrence of stable Pd(IV) compounds is much more rare, however, and kinetic stability of this oxidation state is partially inhibited.

In addition to providing a stable Pd(III) ion, the $Pd([9]aneN_3)_2^{2+}$ ion provides an unusual example of ligand fluxionality that has been discussed elsewhere.[9] Such behavior of this molecule is indicative of the considerable room-temperature lability of the apical amines, which leads to protonation of the $Pd([9]aneN_3)_2$ complex in both the +II and +III oxidation states. These results contrast with the $Ni([9]aneN_3)_2^{n+}$ complexes, where no stable protonated species have been identified. Zompa has studied the protonated complexes of $Pd([9]aneN_3)_2^{2+}$ independently and has provided crystallographic evidence for both the mono- and diprotonated species.[10]

Through the use of ESR spectroscopy a number of examples of Pd(III) species, generated primarily by irradiation, have been detected.[11] There is also a recent report of Pd^{3+} in CaO where the ion was identified directly in the crystalline matrix.[11d] Pd(III) has been suggested as the oxidation state of a number of Pd(dithiolene)$_2$ and Pd(tetrathiolate)$_2$ complexes[12] where electron delocalization has been invoked to explain the appearance of the unusual palladium centers. Molecular orbital calculations[12b] based upon ESR spectroscopic data place the actual spin density at the palladium atom as low as 25%. More recently, Schroder et al.[13] have synthesized the 1,4,7-trithiacyclononane ligand and have

(1) (a) Zang, R.; Zompa, L. J. *Inorg. Chem.* **1976**, *15*, 1499. (b) Margulis, T. N.; Zompa, L. J. *Inorg. Chim. Acta* **1978**, *28*, L157. (c) McAuley, A.; Norman, P. R.; Olubuyide, O. *J. Chem. Soc., Dalton Trans.* **1984**, 1501. (d) Wieghardt, K.; Walz, W.; Nuber, B.; Weiss, J.; Ozarowski, A.; Stratemeier, H.; Reinen, D. *Inorg. Chem.* **1986**, *25*, 1651.
(2) (a) Kuppers, H. J.; Neves, A.; Pomp, C.; Ventur, D.; Wieghardt, K.; Nuber, B.; Weiss, J. *Inorg. Chem.* **1986**, *25*, 2400. (b) Koyama, H.; Yoshino, T. *Bull. Chem. Soc. Jpn.* **1975**, *45*, 481.
(3) (a) Wieghardt, K.; Schmidt, W.; Herrmann, W.; Kuppers, H. J. *Inorg. Chem.* **1983**, *22*, 2953. (b) Boeyens, J. C. A.; Forbes, A. G. S.; Hancock, R. D.; Wieghardt, K. *Inorg. Chem.* **1985**, *24*, 2926.
(4) Wieghardt, K.; Hermann, W.; Koppen, M.; Jibril, I.; Huttner, G. *Z. Naturforsch, B: Anorg. Chem., Org. Chem.* **1984**, *39B*, 1335.
(5) Wieghardt, K.; Koppen, M.; Swirdoff, W.; Weiss, J. *J. Chem. Soc., Dalton Trans.* **1983**, 1869.
(6) Hartley, F. R. *The Chemistry of Platinum and Palladium*; Applied Science Publishers: London, 1973.
(7) (a) Mertes, K. B. *Inorg. Chem.* **1978**, *17*, 49. (b) Ito, T.; Ito, H.; Toriumi, K. *Chem. Lett.* **1981**, 1101.
(8) Fortier, D.; McAuley, A.; Subramanian, S.; Whitcombe, T. W. Presented at the 30th International Congress of Pure and Applied Chemistry, September, 1985, Manchester, U.K.
(9) Hunter, G.; McAuley, A.; Whitcombe, T. W. *Inorg. Chem.*, in press.
(10) Zompa, L. J., personal communication.
(11) (a) Krigas, T.; Rogers, M. T. *J. Chem. Phys.* **1971**, *54*, 4769. (b) Eachus, R. S.; Graves, R. E. *J. Chem. Phys.* **1976**, *65*, 5445. (c) Raizman, A.; Barak, J.; Suss, J. T. *Phys. Rev. B: Condens. Matter* **1985**, *31*, 5716.
(12) (a) Alvarez, S.; Vicenter, R.; Hoffmann, R. *J. Am. Chem. Soc.* **1985**, *107*, 6253. (b) Kirmse, R.; Stach, J.; Dietzsch, W.; Steimcke, G.; Hoyer, E. *Inorg. Chem.* **1980**, *19*, 2679.
(13) (a) Blake, A. J.; Holder, A. J.; Hyde, T. I.; Roberts, Y. V.; Lavery, A. J.; Schroder, M. *J. Organomet. Chem.* **1987**, *323*, 261. (b) Blake, A. J.; Holder, A. J.; Hyde, T. I.; Schroder, M. *J. Chem. Soc., Chem. Commun.* **1987**, 987.

0020-1669/88/1327-3090$01.50/0

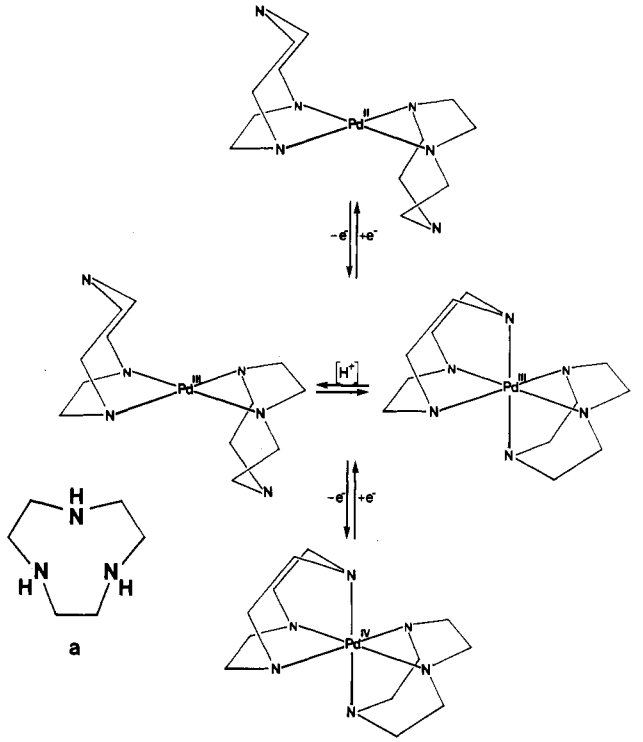

Figure 1. Oxidative interconversions of the relevant $Pd([9]aneN_3)_2^{n+}$ species. Interconversion of the $Pd([9]aneN_3)_2^{3+}$ species between the square-planar and octahedral geometry is through protonation of the apical amines. Also shown (a) is the ligand, 1,4,7-triazacyclononane.

shown that it is also capable of stabilizing Pd and Pt in a +3 oxidation state although, with sulfur as the ligating atom, delocalization is possible. Hawthorne et al.[14] have also observed a Pd(III) oxidation state, using electrochemical methods in their investigation of $Pd(carborane)_2$ complexes.

The $Pd([9]aneN_3)_2^{3+}$ complex described herein represents the first example of a monomeric Pd(III) ion that is stable for very long periods of time in aqueous (pH ≈3–8) solutions. Electrochemical, kinetic, and ESR studies are reported in an examination of the nature of the metal ion in this unusual oxidation state.

Experimental Section

Synthesis. Preparation of the ligand (1,4,7-triazacyclononane) was achieved by a modification of the Richman–Atkins synthesis[15] and has been described previously.[1c]

$PdCl_2$ (0.50 g, 2.8 mmol) was dissolved in 20 mL of deionized water and adjusted to pH ≈9 with NaOH. The high pH prevented all of the solid from dissolving immediately. The solution was warmed to ≈50 °C. The ligand (0.90 g, 7.0 mmol) was added directly to the $PdCl_2$ solution where it dissolved rapidly. Heating was continued for ≈1 h at this temperature, during which time the remaining solid $PdCl_2$ dissolved, yielding a lemon yellow solution with Pd metal being deposited (≈0.13 g or 45%). The metallic solid was removed by filtration. The yellow filtrate contains two species; the major constituent is the $Pd([9]aneN_3)_2^{3+}$ cation with a minor amount of $Pd([9]aneN_3)_2^{2+}$. The ratio between these species is dependent upon the temperature, time, and anaerobic conditions although these have not been examined quantitatively. Addition of a dilute solution of ammonium hexafluorophosphate produced crystals of $[Pd([9]aneN_3)_2](PF_6)_2$, which will be discussed elsewhere.[9] Anal. Calcd for $PdC_{12}H_{30}N_6P_2F_{12}$: C, 22.01; H, 4.62; N, 12.84. Found: C, 22.33; H, 4.97; N, 12.56. Addition of a saturated solution of NH_4PF_6 caused precipitation of the more abundant $[Pd([9]aneN_3)_2](PF_6)_3$ as a yellow powder. Anal. Calcd for $PdC_{12}H_{30}N_6P_3F_{18}$: C, 18.02; H, 3.78; N, 10.51. Found: C, 18.70; H, 3.41; N, 10.25. Aqueous solutions prepared from this material were identical in all respects with those generated by chemical or electrochemical oxidation of the Pd(II) complex. All attempts at recrystallization of the $Pd([9]aneN_3)_2^{3+}$ species with a wide variety of anions and from various solvents and solvent mixtures have failed to produce an X-ray quality crystal although such work is still proceeding.

Solution Chemistry Studies. UV–visible absorption spectra were obtained by using a Perkin-Elmer Lambda 4B spectrophotometer for the normal range (190–900 nm) and on a Cary 17 (Varian) for the near-infrared range (<1300 nm). Measurement of pH was achieved with a glass electrode calibrated against appropriate standard pH buffers. For pH measurement of the solutions used in UV–visible spectra, the solution (3 mL) was transferred to the potentiometric cell.

For the voltammetry studies, the pH electrode was incorporated into the cell and the pH monitored continuously. The experiments were performed with a three-electrode cell connected to a PAR 175 universal programmer equipped with a PAR 174A polarographic analyzer and a Hewlett-Packard 7070A X-Y recorder or with a PAR 273 potentiostat/galvanostat interfaced to an IBM PC computer. Platinum microspheres were employed as both the counter and working electrodes with a saturated calomel electrode as reference. The voltage of the reference electrode was checked periodically by measurement of a known redox couple. The ionic strength of the electrolyte was 1.0 M in the appropriate lithium salt except for the runs in acetate-buffered media where an ionic strength of 0.2 M was used, composed of appropriate amounts of $LiNO_3$, NaOAc, and HOAc.[16]

ESR spectra of the Pd(III) complex were recorded on a Varian E-6S spectrometer using X-band radiation, and the field strength was calibrated with DPPH (g = 2.0037). Solutions of $Pd([9]aneN_3)_2^{3+}$ were obtained directly from the reaction mixture or could be generated via electrochemical or chemical oxidation of the $Pd([9]aneN_3)_2^{2+}$ species. Spectra were observed in a frozen matrix at 77 K and at room temperature.

^1H and ^{13}C NMR spectra of the Pd(II) and Pd(IV) complex were recorded at 250.1 and 69.2 MHz, respectively, with a Bruker WM250 Fourier transform spectrometer locked to the solvent deuterium resonance. ^{13}C spectra were obtained with broad-band irradiation at appropriate frequencies to decouple the proton resonances.

Stopped-Flow Kinetics. The apparatus employed has been previously described.[17] All reactions were monitored under pseudo-first-order conditions at constant temperature (±0.1 °C) by observation of appropriate UV–visible wavelengths, as outlined in the text. The stopped-flow data were collected by an IBM PC computer coupled to a Techmar Labmate A/D convertor. The internal clock was obtained from the Labmate, which had been checked electronically. The reactions were monitored to completion, and the infinity value was derived from the average of the final 25 data points. All reactions were observed to give linear plots for ln (ΔOD) vs time to >5 half-lives, from which the rate could be obtained by standard least squares.

The preparations of $Ni([9]aneN_3)_2^{3+}$,[1c] $Ni(Me[9]aneN_3)_2^{3+}$,[18] $Co([9]aneN_3)_2^{2+}$,[2a] $Co(sep)^{2+}$,[19] and Co^{3+}_{aq}[20] have been described previously. The stoichiometry of all of the cross-reactions was confirmed by spectrophotometric titration of the $Pd([9]aneN_3)_2^{n+}$ species with the appropriate reagent. The ionic strength was controlled by the addition of the appropriate lithium salts. The acetate buffer solutions were similar to those used in the electrochemical experiments. The decomposition of the Ni(III) species has been monitored at appropriate pHs[21] and was found to be not significant (<1%) compared to the rate of cross-reactions. However, Ni(III) solutions at higher pH were prepared by the addition of a solid Ni(III) salt to the buffer immediately prior to the reaction to minimize decomposition.

Results and Discussion

The present synthesis gives a reproducible yield of 55% $Pd([9]aneN_3)_2^{3+}$, which does not appear to be enhanced by longer reaction times or more forcing conditions, although some further oxidation of the residual $Pd([9]aneN_3)_2^{2+}$ complex does occur. Most of the loss of palladium appears to be as Pd metal, the origin of which is probably through a combination of solvent reduction, due to the necessary basicity of the solution, and a disproportionation reaction to give the $Pd([9]aneN_3)_2^{3+}$ cation

$$2Pd([9]aneN_3)_2^{2+} + Pd(H_2O)_4^{2+} \rightarrow 2Pd([9]aneN_3)_2^{3+} + Pd^0$$

Evidence for this pathway is provided by the generation of the Pd(III) species under anaerobic, nonoxidizing conditions in H_2O,

(14) Hawthorne, M. F.; Dunks, G. B. *Science (Washington, D.C.)* **1972**, *178*, 462.
(15) (a) Atkins, T. J.; Richman, J. E.; Oettle, W. F. *Org. Synth.* **1978**, *58*, 86. (b) Atkins, T. J.; Richman, J. E. *J. Am. Chem. Soc.* **1974**, *96*, 2268.
(16) Vogel, A. I. *Quantitative Inorganic Analysis, Theory and Practice*, 2nd Ed., Longmans, Green and Co., Toronto, 1951, pg. 868–70.
(17) Ellis, K. J.; McAuley, A. *J. Chem. Soc., Dalton Trans.* **1973**, 1533.
(18) McAuley, A.; Xu, C.; *Inorg. Chem.* **1988**, *27*, 1204.
(19) Creaser, I. I.; Geue, R. J.; Harrowfield, J. M.; Herlt, A. J.; Sargeson, A. M.; Snow, M. R.; Springborg, J. *J. Am. Chem. Soc.* **1982**, *104*, 6016.
(20) Endicott, J. F.; Durham, W.; Kumar, K. *Inorg. Chem.* **1982**, *104*, 2437.
(21) McAuley, A.; Whitcombe, T. W., unpublished data.

again with the deposition of palladium metal. This reaction also appears to be operative in the generation of the Pd(III) species in nonaqueous solvents (i.e. DMSO). Similar behavior is observed[7] for a number of macrocyclic complexes involving Ag(I) where coordination results in disproportionation to give Ag^{II}(macrocycle) and Ag^0. An enhanced rate of reaction is observed in the presence of air (specifically O_2), which is capable of oxidizing the Pd(II) species since the potential of the $Pd([9]aneN_3)_2^{3+/2+}$ redox couple is relatively low in neutral media. The rate of oxidation to the Pd(III) species may be monitored by UV/visible spectroscopy. Values of 4.7×10^{-4} M^{-1} s^{-1} and 1.6×10^{-4} M^{-1} s^{-1} were obtained for aerobic and anaerobic conditions, respectively. These values are consistent with the electron self-exchange rate for the complex and are indicative of the structural rearrangements necessary between the nominally square-planar Pd(II) and the predominantly octahedral Pd(III) species.

UV–Visible Spectroscopy. The UV–vis spectrum of $Pd([9]aneN_3)_2^{2+}$ has a peak of significant intensity at 296 nm (ϵ = 440 M^{-1} cm^{-1}) with a shoulder at 440 nm (ϵ = 30 M^{-1} cm^{-1}). No other significant absorptions at lower energies were observed. Application of the Tanabe–Sugano diagram[22] for a d^8 ion gives a fit for Dq = 2280 cm^{-1} with B = 1200 cm^{-1}, slightly higher than might be expected for Pd(II) but consistent with the expected strong field generated by the macrocyclic ligand.

The corresponding spectrum of the Pd(III) species is not as easily interpreted since the molecule is d^7 and hence orbitally degenerate, which results in a Jahn–Teller distortion. On the basis of the corresponding Ni(III) complex[1] and the ESR spectra of the Pd(III) species, the ground state is probably $^2A_{1g}$. The presence of only two peaks in the spectrum at 383 nm (ϵ = 590 M^{-1} cm^{-1}) and at 314 nm (ϵ = 1240 M^{-1} cm^{-1}) does not provide sufficient information to determine the extent of the Jahn–Teller distortion. A further band at 196 nm ($\epsilon = 1.12 \times 10^4$ M^{-1} cm^{-1}) is due to charge transfer, and there are no low-energy absorptions.

The Pd(IV) species exhibits a single absorption band at 450 nm (ϵ = 860 M^{-1} cm^{-1}) due to the first spin-allowed transition from the $^1A_{1g}$ ground state. Assuming the energy of this transition (22 220 cm^{-1}) represents $10Dq$, a value of 2222 cm^{-1} may be assigned to Dq, giving a value of 1300 cm^{-1} for B. The $Pd([9]aneN_3)_2^{4+}$ species was generated by the chemical oxidation of the Pd(III) species through a spectrophotometric titration that allowed for the confirmation of the concentration of both species. Unfortunately, the Pd(IV) species is not isolable since it decomposes with time. The decomposition has been observed in both the UV–vis and NMR spectra.

ESR Spectroscopy. For Pd^{3+} (d^7) in an octahedral environment, the expected electron configuration is low spin with the single electron occupying either a d_{z^2} or a $d_{x^2-y^2}$ orbital. As the ground state is nominally orbitally degenerate, a Jahn–Teller distortion is anticipated. However, at 77 K[23] in neutral media of low ionic strength (μ < 0.01 M), the ESR spectrum obtained is an isotropic signal centered at g_{iso} = 2.077. This species is stable and the presence of an ESR spectrum has been recorded after 2 years with no significant loss in intensity. With an increase in the ionic strength or a decrease in the pH of the solution, an anisotropic ESR spectrum is observed with $g_\perp = 2.115_8$ and $g_\parallel = 2.007_3$ ($A_\parallel$ = 26.2 G). This is due to ion-pair formation resulting in a static distortion in the geometry. The spectra are presented in Figure 2.

The hyperfine coupling on the axial component occurs as a quintet (ratio: 1:2:3:2:1) and is indicative of axially coordinated nitrogen nuclei (I = 1) rather than coupling to the spin-active palladium nucleus. There is slight evidence for hyperfine coupling to the ^{105}Pd ($I = {}^5/_2$; 22.2% natural abundance) in two very weak shoulders observed on the equatorial component. The total intensity of these lines relative to the absorptions is expected to be only ≈4.7%, and the coupling is not definitively discernible. This

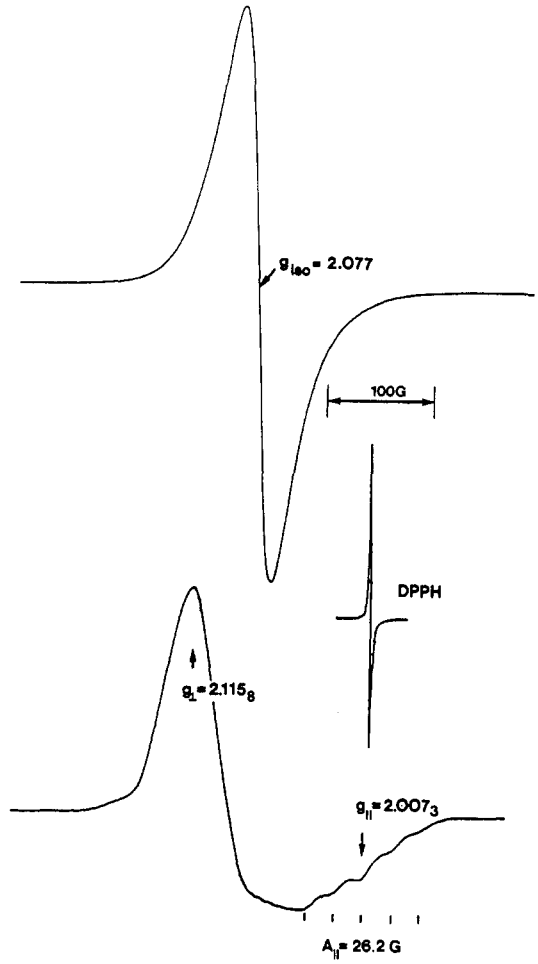

Figure 2. ESR spectra of the $Pd([9]aneN_3)_2^{3+}$ species: (a) ≈1 × 10^{-3} M of $Pd([9]aneN_3)_2(PF_6)_3$ dissolved in deionized water; (b) ≈1 × 10^{-3} M of $Pd([9]aneN_3)_2(PF_6)_3$ dissolved in deionized water saturated with Li_2SO_4.

contrasts with recent work by Schroder et al.[13] on the sulfur analogue of $[9]aneN_3$ where coupling to the Pd nucleus was reported on both axial and equatorial components.

The sequence $g_\perp > g_\parallel = g_e$ (g_e (free electron value) = 2.0023) is compatible with a $^2A_{1g}$ (d_{z^2}) ground state, suggesting that the structure undergoes a tetragonal elongation in acidic/ionic media. The presence of both isotropic and anisotropic patterns suggests that the compound is dynamically Jahn–Teller distorted at low ionic strengths. Equations for the value of g under both conditions have been given[24]

$$g_\parallel = g_e + 2(\lambda^2/\delta^2) = g_e + 2\mu' \quad (1)$$

$$g_\perp = g_e + 3\lambda[1.38/E_3 + 0.62/E_4] + 2(\lambda^2/\delta^2) = g_e + 6\mu + 2\mu' \quad (2)$$

and

$$g_{iso} = {}^2/_3 g_\perp + {}^1/_3 g_\parallel = g_e + 2\lambda[1.38/E_3 + 0.62/E_4] + 2(\lambda^2/\delta^2) \quad (3)$$

where λ is the effective spin–orbit coupling constant, δ is the energy separation between the low-spin ground state ($^2A_{1g}$) and the first excited state (the split level of the octahedral $^4T_{1g}$ parent state), and E_3 and E_4 are the transitions from the ground state to the $^2_aT_{2g}$ and $^2_bT_{2g}$ parent states. Using the above equations with values of E_3 = 37 700 cm^{-1} and E_4 = 46 600 cm^{-1} together with a reduced spin–orbit coupling parameter of 720 cm^{-1}, we obtain a good fit to the above equations. The second-order correction (μ') is particularly small in this molecule, suggesting that the first excited state is ≈13 700 cm^{-1} above the ground state. The magnitude of

(22) Tanabe, Y.; Sugano, S. *J. Phys. Soc. Jpn.* **1954**, *9*, 753, 766.
(23) The $Pd([9]aneN_3)_2^{3+}$ complex gives a broad isotropic signal at room temperature in aqueous solution using a quartz flat cell, centered at g_{iso} = 2.08.
(24) LaCroix, R.; Hochli, U.; Muller, K. A. *Helv. Phys. Acta.* **1964**, *37*, 627.

this parameter is consistent with the observation of only the spin-paired configuration in complexes of the second-row transition elements.

The reduction in the spin–orbit coupling parameter from the free-spin value has often been used as a measure of the covalency of the metal–ligand bonds.[25] For Pd(III), $\lambda_c = 1640$ cm^{-1} where the spin–orbit coupling parameter has been calculated from a linear extrapolation of the value for the lower valences.[26] The covalency parameter, K, is determined from[25]

$$\lambda = K^2\lambda_c \quad (4)$$

and in this case, $K = 0.66$. This value is typical of second- and third-row transition elements where the degree of covalency in the metal–ligand bond is expected to be greater than that for first-row elements. For comparison, the Ni([9]aneN$_3$)$_2^{3+}$ complex has recently been studied[1d] and found to have an effective spin–orbit coupling parameter of 450 cm^{-1}, which gives $K = 0.8$.

An alternate method for determining the degree of covalency is through the detection of hyperfine coupling of the electron to the ligand nuclei in cases where the nuclei have a nonzero nuclear angular moment.[27] It has been observed in complexes of Pd(III) with dithiolenes and tetrathiolates that extensive delocalization of the single electron onto the ligand occurs. This results in low (≈25%) spin density at the palladium,[12b] and such structures have sometimes been viewed as coordinated ligand radicals. The delocalization results in narrow ESR lines and large coupling constants to ligand nuclei. With the complex under study, the ligating nitrogens do not have energetically accessible d orbitals nor are they involved in a π-bonded system, and thus, the amines act as pure σ-donors.[25] Electron delocalization must occur through the antibonding molecular orbital and through dipolar interaction. The axial coupling constant observed in this complex ($A_\parallel = 26.2$ G) is, to first order, isotropic; hence, from a knowledge of the isotropic contact field provided by the nitrogen nucleus (550 G),[28] a value of ≈4.7% is obtained. This value is consistent with the value of ≈3.4% obtained for Ni([9]aneN$_3$)$_2^{3+}$ from a hyperfine coupling constant of 19 G. Both of these values may be used to calculate the expected value of K since $K = 1 - 6(\alpha)$ where α represents the delocalization of the electron onto the ligand. For the Ni(III) species, $K = 0.796$, which is in excellent agreement with the value obtained from the reduction of the spin–orbit parameter. For Pd(III), $K = 0.718$, which is slightly higher than the value obtained from the spin–orbit parameter.

This slight difference can probably be attributed to contributions from two factors. The first is the simplicity of approach used in calculating the extent of electron overlap on the ligand. Terms arising from overlap into the p orbital and consideration of the sp^3 hybridization of the nitrogen orbitals will result in an effectively lower contact term and, hence, a larger electron delocalization. Single-crystal ESR spectroscopy will provide for a better determination of all the relevant parameters, particularly with respect to the anisotropic contribution to electron delocalization from which the extent of p-orbital involvement can be determined.

The second factor is the nature of the observed ESR spectrum. Both $g_\perp$ and $g_\parallel$ are close together and similar to g_e. This results in a perturbation of the observed spectral line shape, resulting in the measured g values being slightly less than the true values. Increasing the measured values would result in a slightly larger covalency parameter. The spectroscopic line shape is also affected by the dynamic Jahn–Teller distortion since the anisotropicity arises from a static conformation and the maximum $g_\perp$ will occur only for a static structure.

The structure of the ligand in Pd([9]aneN$_3$)$_2^{3+}$ thus prevents extensive delocalization of the electron, which is in contrast to a number of Pd(III)–sulfur complexes.[12,13] The magnetic anisotropy and ligand hyperfine coupling reinforce the conclusion that the electron is essentially localized on the metal center. A number of other Pd(III) complexes (specifically Pd(Me[9]aneN$_3$)$_2^{3+}$, Pd([10]aneN$_3$)$_2^{3+}$, Pd([9]aneN$_2$S)$_2^{3+}$, and Pd(cyclam)$^{3+}$) have been generated in our laboratory and, for a similar analysis of the spectra, support the presence of a metal-centered radical.

Table I. Parameters[a] Obtained from Calculated ^{1}H NMR Spectra in D_2O

	Pd^{II}([9]aneN$_3$)$_2$	Pd^{IV}([9]aneN$_3$)$_2$	Co^{III}([9]aneN$_3$)$_2$
$\delta_1 = \delta_3$	3.41	3.90	3.14
$\delta_2 = \delta_4$	2.95	3.62	2.88
$J_{12} = J_{34}$	−14.4	−12.1	−11.7
$J_{13} = J_{24}$	3.9	7.1	7.7
$J_{14} = J_{23}$	7.5	7.0	6.8

[a] Chemical shifts in ppm; coupling constants in Hz.

^{1}H and ^{13}C NMR. Oxidation of the Pd([9]aneN$_3$)$_2^{2+}$ species was achieved in D_2O under neutral conditions by the addition of $Na_2S_2O_8$. The reaction was carried out in an NMR tube with a 0.28 M Pd(II) solution in 3 mL of solvent. Four half-equivalents of $Na_2S_2O_8$ were added consecutively to give complete oxidation to the Pd(IV) with a first "endpoint" being observed after 1 equiv, as expected. This feature is observed as a minimum in the ^{1}H and ^{13}C NMR signals (see Figure 3) and, by the use of ESR spectroscopy to follow the same reaction, as a maximum in the ESR signal intensity. (Slight differences in the $S_2O_8^{2-}$ concentration resulted in residual peak intensity at the "endpoint".) After a further 3 h, the peak height for the Pd(IV) complex was seen to be enhanced, giving evidence for the slow reaction rate observed. The NMR spectra was also obtained after 1 and 8 days (spectrum g, Figure 3), and the appearance of new peaks in both the ^{1}H and ^{13}C NMR spectra during this time demonstrated the instability of the Pd(IV) compound. Assignment of all the new resonances was not undertaken, but resonances associated with the Pd(II) complex were identified. The absence of any ESR-active species, suggests that the Pd(III) species was not part of the decomposition pathway.

An interesting feature of the ^{1}H NMR spectra is the effect of oxidation upon the protonated solvent peak at ≃4.7 ppm. The signal broadens and goes through a minimum concurrent with the production of the paramagnetic Pd(III) ion. This is due to the interchange of the solvent molecules in the second solvation sphere, which are paramagnetically shifted, with the bulk solvent molecules. No calculations of the residence time have been attempted.

Neither the Pd(II) species nor the Pd(III) species, when kept in sealed NMR and ESR tubes, respectively, showed any sign of oxidation or decomposition over extended periods of time.

The ^{1}H and ^{13}C NMR spectra for Pd([9]aneN$_3$)$_2^{2+}$ were not those expected for a square-planar complex and provide evidence for the fluxionality of the macrocyclic ligand. The mechanistic interpretation is based on the pseudo-inner-sphere substitution of the apical nitrogen onto the palladium(II) ion. Variable-temperature ^{13}C NMR studies in CD_3OD gave a value of 10.2 ± 3.8 kcal/mol for ΔG^*_{298}.

The coupling constants and chemical shifts of the ^{1}H NMR spectrum for the Pd(II) species are given in Table I together with the coupling constants for the Pd(IV) species and for Co([9]aneN$_3$)$_2^{3+}$, which has been observed by Wieghardt et al.[2a] The NMR spectra for the Pd(IV) species are as expected. A single signal is observed in the ^{13}C spectrum, which is shifted to slightly higher frequencies, compared to that of the Pd(II) complex, due to the rigidity of the conformation and the octahedral coordination. Indeed, the observed chemical shift matches well the chemical shift for the carbons in the chelating ethylene bridge of the Pd(II) complex. The ^{1}H NMR spectrum reflects the increase in charge at the palladium, being shifted to slightly higher frequencies particularly with respect to the d^6 Co analogue. However, the values obtained for the coupling constants suggest a close analogy

(25) (a) Figgis, B. N. *Introduction to Ligand Field Theory*; Wiley: Toronto, Canada, 1966. (b) Gerloch, M.; Miller, J. R. *Prog. Inorg. Chem.* **1970**, *10*, 1.
(26) Dunn, T. M. *Trans. Faraday. Soc.* **1961**, *57*, 1441.
(27) Abragam, A.; Bleaney, A. *Electron Paramagnetic Resonance of Transition Ions*; Clarendon: Oxford, England, 1970.
(28) Atkins, P. W.; Symons, M. C. R. *The Structure of Inorganic Radicals*; Elsevier: London, 1967, p 21.

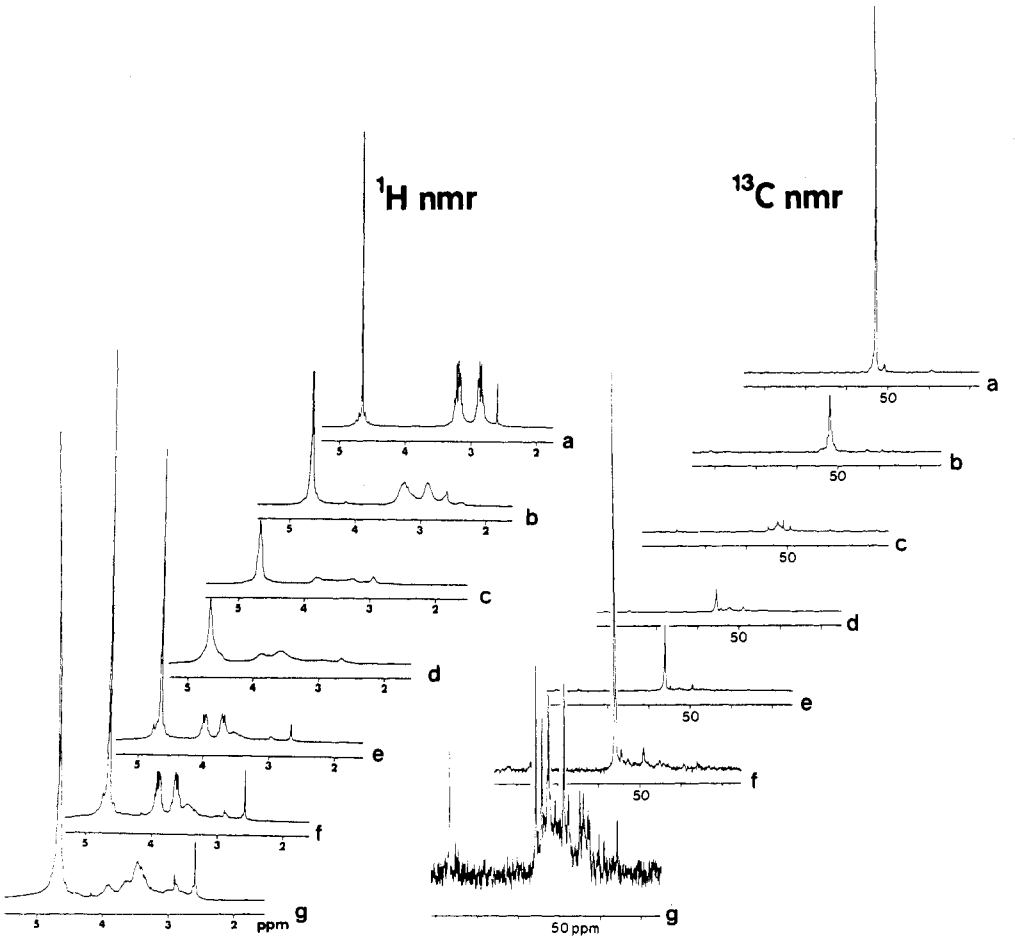

Figure 3. ^{1}H and ^{13}C NMR spectra of Pd([9]aneN$_3$)$_2^{n+}$ during oxidative titration with $Na_2S_2O_8$: (a) 0 molar equiv; (b) $^1/_2$ equiv; (c) 1 equiv; (d) $1^1/_2$ equiv; (e) 2 equiv; (f) 2 equiv after 3 h; (g) 2 equiv ≈8 days. The ^{1}H and ^{13}C NMR spectra at 1 equiv show slight residual peaks due to a slight excess of oxidant (≈5%). The ^{1}H resonances of the Pd(II) complex appear at ≈2.7 and ≈3.3 ppm. These signals disappear with oxidation (spectrum c) to Pd(III). Signals due to the Pd(IV) species are observable at ≈3.6 and ≈4.0 ppm in the final spectrum.

between the structure of the two compounds; hence, the Pd(IV) structure is confirmed as octahedral.

Electrochemistry. The redox properties of the Pd([9]aneN$_3$)$_2^{n+}$ complex have been examined in aqueous media by cyclic voltammetry over a wide range of pHs. Cyclic voltammetry measures the half-wave potential, $E_{1/2}$, of a reaction and provides information on the reversibility of the electron-transfer process (I_{ox}/I_{red}). The half-wave potential can be related to the formal potential ($E°_{298}$) for the redox process through the Nernst equation

$$E_{1/2} = E°_{298} - \frac{0.5916}{n} \log (D_{ox}/D_{red})^{1/2} \qquad (5)$$

where D_{ox} and D_{red} are the diffusion coefficients of the oxidized and reduced forms of the complex, respectively. If the diffusion coefficients are approximately equal, which is generally the case, then the latter term is comparatively small (≈2–3 mV) and the $E_{1/2}$ value measured is a good approximation of the formal potential.

The Pd([9]aneN$_3$)$_2^{n+}$ cations, unlike the Ni([9]aneN$_3$)$_2^{n+}$ complexes, have an energetically accessible +IV oxidation state, albeit of limited stability. The observed cyclic voltammograms thus exhibit two successive 1e redox waves arising from the $Pd^{3+/2+}$ and $Pd^{4+/3+}$ couples. Typically, the peak-to-peak separation for the waves was ≈65–70 mV, slightly higher than the theoretical value due to uncompensated resistances in the electrochemical cell. The current ratio was nearly unity for both waves in neutral to slightly acidic media, indicating good reversibility under these conditions. A typical cyclic voltammogram is provided in Figure 4.

Both the Pd([9]aneN$_3$)$_2^{2+}$ and Pd([9]aneN$_3$)$_2^{3+}$ cations are susceptible to protonation in acidic media to give mono- and diprotonated species. For the Pd(II) species, the first pK_a was

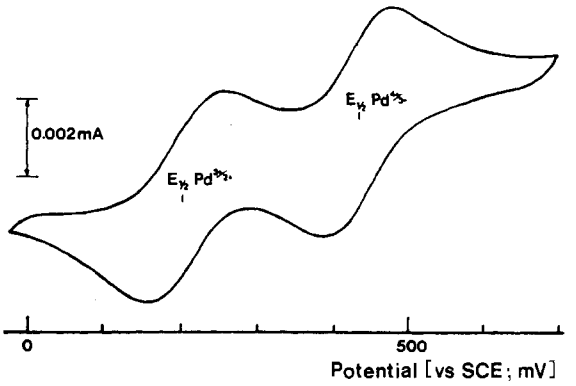

Figure 4. Cyclic voltammogram of Pd([9]aneN$_3$)$_2^{n+}$ in 1.0 M $LiClO_4$ media at pH ≈4.6. Potentials are with respect to NHE. The cyclic voltammogram shows two distinct 1e redox waves corresponding to the $Pd^{3+/2+}$ and $Pd^{4+/3+}$ couples.

determined to be ≈4.7 from kinetic data. This value is much lower than the first pK_a of the free ligand (≈11),[31] being closer to the pK_a for the diprotonated ligand as expected from electrostatic considerations. A second pK_a is determinable from the kinetic data at ≈2.4 but this value is of low precision owing to limited data. For the Pd(III) species, pK_a's at 4.45 and 3.17 have been determined by potentiometry. The speciation of the Pd([9]aneN$_3$)$_2^{n+}$ cations associated with the various protonated forms may be observed from the dependence of the observed electrode potential ($E_{1/2}$) upon the pH of the solution, as shown in Figure 5.

At very low pH's, the reversibility of the $Pd^{3+/2+}$ couple diminishes owing to a decreased stability of the Pd(II) species under

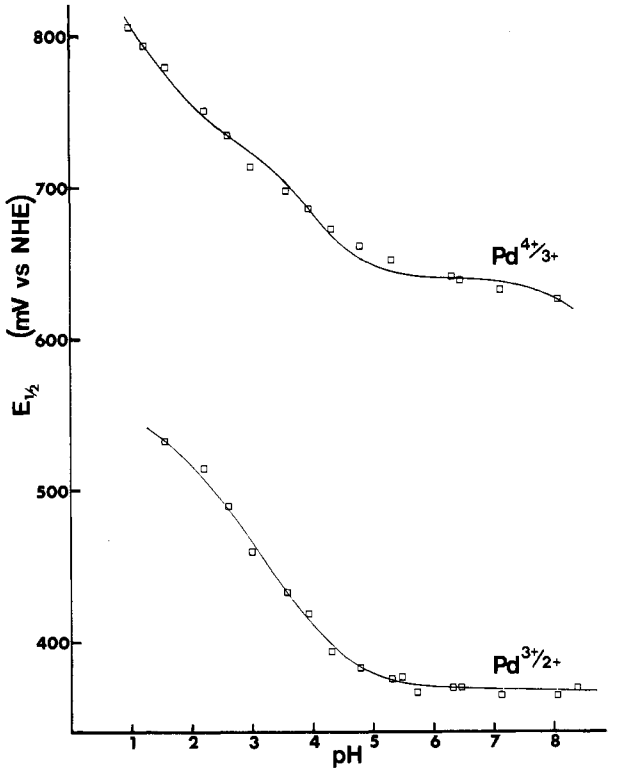

Figure 5. Plot of the measured and calculated $E_{1/2}$ values for the $Pd^{3+/2+}$ and $Pd^{4+/3+}$ couples in perchlorate media. The observed potentials are indicated by a square, which represents an error bar of ±2 mV. The lines are calculated from the equations given in the text.

acidic conditions. Similarly, the $Pd^{4+/3+}$ couple is not observed at high pH's, due to deprotonation and subsequent oxidation of the ligand. A $Pd^{3+/2+}$ wave can be observed at pH's greater than ≈9 with good reversibility so that the complex is a mild oxidant under basic conditions, which is in contrast to macrocyclic complexes of nickel. However, at very high pH, a deprotonation is identified that leads to a lower $E_{1/2}$ value. This facilitates the oxidation of the Pd(II) species to Pd(III) under the synthesis conditions (pH ≈11).

Flat regions (Figure 5) in the $E_{1/2}$ vs pH plots between pH 6 and 8 can be attributed to reaction of the nonprotonated complexes for both oxidation states and the $E_{1/2}$ value (E_I) for this couple can be obtained directly. All of the other potentials afforded by the variety of protonated species, as given in Scheme I, were obtained from computer-assisted simulation of the $E_{1/2}$ vs pH plots using the known values of K_A, K_B, and $K_{B'}$.

The simulation of the potentials was based upon the following system of equations obtained from the appropriate substitutions into the Nernst equation.

$$E_{1/2}(\mathrm{I}) = E_{\mathrm{I}} + 0.05916 \log (\mathrm{KAA/KBB}) \quad (6a)$$

$$E_{1/2}(\mathrm{II}) = E_{\mathrm{II}} + 0.05916 \log (K_B(\mathrm{KAA})/\mathrm{KBB}) \quad (6b)$$

$$E_{1/2}(\mathrm{III}) = E_{\mathrm{III}} + 0.05916 \log (K_B K_{B'}(\mathrm{KAA})/\mathrm{KBB}) \quad (6c)$$

$$E_{1/2}(\mathrm{IV}) = E_{\mathrm{IV}} + 0.05916 \log (\mathrm{KAA}/K_A(\mathrm{KBB})) \quad (6d)$$

$$E_{1/2}(\mathrm{V}) + 0.05916 \log (K_B(\mathrm{KAA})/K_A(\mathrm{KBB})) \quad (6e)$$

$$E_{1/2}(\mathrm{VI}) = E_{\mathrm{VI}} + 0.05916 \log (K_B K_{B'}(\mathrm{KAA})/K_A(\mathrm{KBB})) \quad (6f)$$

$$E_{1/2}(\mathrm{VII}) = E_{\mathrm{VII}} + 0.05916 \log (\mathrm{KAA}/K_A K_{A'}(\mathrm{KBB})) \quad (6g)$$

$$E_{1/2}(\mathrm{VIII}) = E_{\mathrm{VIII}} + 0.05916 \log (K_B(\mathrm{KAA})/K_A K_{A'}(\mathrm{KBB})) \quad (6h)$$

$$E_{1/2}(\mathrm{IX}) = E_{\mathrm{IX}} + 0.05916 \log (K_B K_{B'}(\mathrm{KAA})/K_A K_{A'}(\mathrm{KBB})) \quad (6i)$$

Scheme I

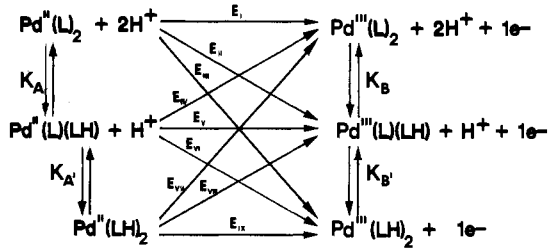

Table II. Electrode Potentials for the $Pd([9]aneN_3)_2^{3+/2+}$ Couple in Various Media

potentials[a]	$Pd([9]aneN_3)_2^{3+}$ perchlorate[b]	$Pd([9]aneN_3)_2^{2+}$ nitrate[c]	$Pd([9]aneN_3)_2^{2+}$ acetate/nitrate[d]
E_I	369.4	368.4	398.5
E_{II}	479	547	567
E_{III}	515	565	595
E_{IV}	450	490	463
E_V	404	427	462
E_{VI}	326	354	382
E_{VII}[e]			
E_{VIII}	698	702	730
E_{IX}	546	570	600
ΔE	2.74	2.17	3.77

[a] The potentials are as defined in the text by eq 6a–i. All potentials are given in mV vs NHE. Details of potentials at individual pH's are provided in supplementary Table I(S). [b] $Pd^{III}([9]aneN_3)_2(ClO_4)_3$ in 1.0 M $LiClO_4$. [c] $Pd^{II}([9]aneN_3)_2Cl_2$ in 1.0 M $LiNO_3$. [d] $Pd^{II}([9]aneN_3)_2Cl_2$ in 0.2 M HOAc/NaOAc/$LiNO_3$. [e] This potential is undefined by the data.

KAA = $(1 + K_A[H^+] + K_A K_{A'}[H^+]^2)$ and KBB = $(1 + K_B[H^+] + K_B K_{B'}[H^+]^2)$, and the equilibrium constants are defined as association constants

$$K_A = [Pd^{II}(L)(LH)]/[Pd^{II}(L)_2][H^+] \quad (7a)$$

$$K_{A'} = [Pd^{II}(LH)_2]/[Pd^{II}(L)(LH)][H^+] \quad (7b)$$

$$K_B = [Pd^{III}(L)(LH)]/[Pd^{III}(L)_2][H^+] \quad (7c)$$

$$K_{B'} = [Pd^{III}(LH)_2]/[Pd^{III}(L)(LH)][H^+] \quad (7d)$$

with L and LH representing the non- and monoprotonated coordinated ligand.

Since proton transfer is diffusion controlled in aqueous media, the above potentials combined to give a single observable $E_{1/2}$ value

$$E_{1/2} = (1/(\mathrm{KAA})\mathrm{KBB})(E_{1/2}(\mathrm{I}) + (E_{1/2}(\mathrm{II}))K_B[H^+] + (E_{1/2}(\mathrm{III}))K_B K_{B'}[H^+]^2) + (K_A[H^+]/(\mathrm{KAA})\mathrm{KBB})(E_{1/2}(\mathrm{IV}) + (E_{1/2}(\mathrm{V}))K_B[H^+] + (E_{1/2}(\mathrm{VI}))K_B K_{B'}[H^+]^2) + (K_A K_{A'}[H^+]^2/(\mathrm{KAA})\mathrm{KBB}) \times (E_{1/2}(\mathrm{VII}) + (E_{1/2}(\mathrm{VIII}))K_B[H^+] + (E_{1/2}(\mathrm{IX}))K_B K_{B'}[H^+]^2) \quad (8)$$

Given E_I, K_A, K_B, and $K_{B'}$, an analysis of the $Pd^{3+/2+}$ redox potentials using the above scheme and eq 8 was carried out by partial computer iteration for the various unknown potentials and the second protonation constant, $K_{A'}$, for the Pd(II) species. The resulting values are tabulated in Table II. The observed and calculated values for $E_{1/2}$ are contained in the supplementary Table I(S). The "goodness of fit" was judged from the absolute average difference between the observed and calculated potentials. The conventional correlation coefficient, r^2, was calculated from a plot of the final calculated $E_{1/2}$ values vs $E_{1/2}$ observed. For all of the media, values better than 0.98 with slopes of unity were obtained, indicating the excellent fit between the experimental points and the curve described by eq 8. Only in the case of the acetate-buffered media were the potentials not overdetermined by the available data.

Scheme II

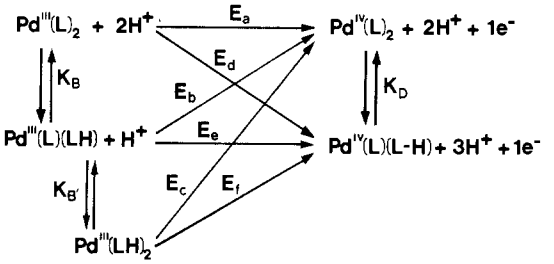

The second protonation constant, $K_{a'} = 6 \times 10^{-3}$ M, for the Pd(II) species, was obtained from all three sets of electrochemical data. It is in excellent agreement with the value of 4×10^{-3} M obtained from kinetic data. The E_{VII} potential was not evaluated since it was found to have no measurable effect upon the calculated potential and, hence, could not be determined.

The potentials derived describe a consistent picture. Generally, an increase in the potentials is observed in going from perchlorate to nitrate to acetate/nitrate media. This may be attributed to the formation of ion pairs between the pendant-protonated amine and the anion. The E_I potential is not significantly affected by the change in media since it involves the nonprotonated species, although a slight increase (≈30 mV) is observed in acetate media. This may be due to the decreased ionic strength ($\mu = 0.2$ M) used for this study.

The increase in potential for the series

$$Pd(L)_2^{3+/2+} < Pd(L)(LH)^{4+/3+} < Pd(LH)_2^{5+/4+}$$

is as expected since the stability of the protonated complexes is less than that of the nonprotonated species. Zompa[10] has recently obtained the crystal structure of the diprotonated Pd(II) complex, suggesting the complex is of reasonable thermodynamic stability. We have independent crystallographic evidence[29] to suggest that the Pd(III) complex may also exist in the diprotonated form in the solid state.

The occurrence of the calculated E_{VI} value at a lower potential than E_I suggests that at lower pHs this pathway will play a significant role in the oxidation of the Pd(II) complexes.

Unlike the Pd(II) or Pd(III) species, the $Pd([9]aneN_3)_2^{4+}$ ion is octahedral as observed by ^1H and ^{13}C NMR and not susceptible to protonation. The pH dependence under acidic conditions for the $Pd^{4+/3+}$ couple originates from the Pd(III) species. However, unlike the $Pd^{3+/2+}$ electrochemistry, the $E_{1/2}$ vs pH plot does not plateau in the pH 6–8 range, as seen in Figure 5. The decreasing potential in this region may be attributed to the deprotonation of the ligand as described in Scheme II. The loss of a proton from a coordinated amine may also contribute to the decomposition of the Pd(IV) species at high pH and to the irreversibility of the electron-transfer process.

The $E_{1/2}$ values observed may be analyzed by using a system of equations similar to those for the $Pd^{3+/2+}$ couple. The equilibrium constants for the Pd(III) species are designated K_B and $K_{B'}$ to be consistent with the $Pd^{3+/2+}$ electrochemistry and $(1 + K_B[H^+] + K_BK_{B'}[H^+]^2)$ has been replaced by KBB and $(1 + K_D[H^+])$ by KDD.

$$E_{1/2}(a) = E_a + 0.05916 \log ((KBB)K_D[H^+]/KDD) \quad (9a)$$

$$E_{1/2}(b) = E_b + 0.05916 \log ((KBB)K_D[H^+]/K_B(KDD)) \quad (9b)$$

$$E_{1/2}(c) = E_c + 0.05916 \log ((KBB)K_D/K_BK_{B'}(KDD)) \quad (9c)$$

$$E_{1/2}(d) = E_d + 0.05916 \log ((KBB)[H^+]/KDD) \quad (9d)$$

$$E_{1/2}(e) = E_e + 0.05916 \log ((KBB)[H^+]/K_B(KDD)) \quad (9e)$$

$$E_{1/2}(f) = E_f + 0.05916 \log ((KBB)[H^+]/K_BK_{B'}(KDD)) \quad (9f)$$

(29) McAuley, A.; Whitcombe, T. W., unpublished data.

Table III. Electrode Potentials for the $Pd([9]aneN_3)_2^{4+/3+}$ Couple in Various Media

potentials[a]	$Pd([9]aneN_3)_2^{3+}$ perchlorate[b]	$Pd([9]aneN_3)_2^{2+}$ nitrate[c]	$Pd([9]aneN_3)_2^{2+}$ acetate/nitrate[d]
E_a	640	639	600
E_b	911	920	928
E_c	865	872	870
E_d	1079	1144	728
E_e[e]			
E_f[e]			
K_d, M	1×10^{-9}	1×10^{-9}	1×10^{-7}
ΔE	3.98	5.54	1.59

[a] The potentials are as defined in the text by eq 9a–f. All potentials are in mV vs NHE. Details of potentials at individual pH's are provided in supplementary Table II(S). [b] $Pd^{III}([9]aneN_3)_2(ClO_4)_3$ in 1.0 M $LiClO_4$. [c] $Pd^{II}([9]aneN_3)_2Cl_2$ in 1.0 M $LiNO_3$. [d] $Pd^{II}([9]aneN_3)_2Cl_2$ in 0.2 M HOAc/NaOAc/$LiNO_3$. [e] These potentials are undefined by the data.

These equations can be combined into a single equation for calculating the observable potential

$$E_{1/2} = (K_D/(KDD)KBB)(E_{1/2}(a) + K_B[H^+]E_{1/2}(b) + K_{BKB'}[H^+]^2E_{1/2}(c)) + (1/(KDD)KBB)(E_{1/2}(d) + K_B[H^+]E_{1/2}(e) + K_BK_{B'}[H^+]^2E_{1/2}(f)) \quad (10)$$

The results obtained from the analysis of the data using eq 10 are tabulated in Table III. The observed and calculated values for $E_{1/2}$ are contained in the supplementary Table II(S).

The equilibrium constants used for the Pd(III) species are those shown above. These values form a common link between the two electrochemical schemes. The deprotonation constant, K_d, was obtained by using the iterative route outlined above. Modification of the equation for the $E_{1/2}(c)$ potential was necessary to accommodate the observed slope of the $E_{1/2}$ vs pH plot in the low-pH region and is attributable to a slow proton transfer. A similar slow-proton-transfer equilibrium for a nitrogen apically bound to a d^7 ion has been observed by Fabrizzi et al.[30] for Ni(scorpiand)$^{3+}$.

The electrochemical potentials calculated by using eq 10 do not allow for the determination of E_e or E_f since they do not affect the calculated value. However, the other potentials describe a consistent picture of the electrochemical pathways for the $Pd^{4+/3+}$ couple, with little variation in potentials E_a, E_b, and E_c between the three media. This might be as expected since close-ion-pair formation with the protonated amine would be limited to the Pd(III) species and thus is not as significant. The potential for the deprotonated species, E_d, is subject to greater uncertainty owing to the minimal influence this potential has on the calculated data. The potential is derived from the slope of the plot above pH 7 and is heavily influenced by the choice of K_d. Further work on the electrochemistry of the $Pd^{4+/3+}$ couple at high pH's will provide better insight into the nature of the deprotonation step for these species.

Electron-Transfer Kinetics. Oxidation of $Pd([9]aneN_3)_2^{2+}$. This has been studied in reactions using $Ni([9]aneN_3)_2^{3+}$ and $Ni(Me[9]aneN_3)_2^{3+}$ ($Me[9]aneN_3$ = 2-methyl-1,4,7-triazacyclononane) in acetate-buffered solution. The reactions were conducted under pseudo-first-order conditions with the Pd(II) cation in excess. This was necessary to minimize the subsequent oxidation, by Ni(III), of the Pd(III) formed during the oxidations. The appearance of the Pd(III) absorption at $\lambda = 380$ nm was used to monitor the reaction. The rate constants for the oxidations are provided in Table IV, and a plot of k_{obsd} and k_{calcd} vs pH for the reaction with $Ni([9]aneN_3)_2^{3+}$ is provided in Figure 6. The kinetic data and a plot of k_{obsd} and k_{calcd} vs pH for $Ni(Me[9]aneN_3)_2^{3+}$

(30) Pallavinci, P. S.; Perotti, A.; Poggi, A.; Seghi, B.; Fabbrizzi, L. *J. Am. Chem. Soc.* **1987**, *109*, 5139.

Table IV. Rate Constants for Reactions of $Pd([9]aneN_3)_2^{n+}$

		rate[a]	E^b	k_{11}[a]	k_{22}(calcd)[a]
		Pd^{II} to Pd^{III}			
$Ni([9]aneN_3)_2^{3+}$	k_1	2060 ± 75	0.547	6000	3.2×10^{-6}
	k_2	120 ± 100	0.483	6000	7.5×10^{-8}
	k_3	50 ± 50	0.345	6000	
$Ni(Me[9]aneN_3)_2^{3+}$	k_1	1800 ± 70	0.557	6100	1.7×10^{-6}
	k_2	96 ± 70	0.493	6100	3.3×10^{-8}
	k_3	"30"	0.355	6100	
		Pd^{III} to Pd^{II}			
$Co(sep)^{2+}$	k_1	560 ± 100	0.698	5.1	1.9×10^{-6}
$Co(non)_2^{2+}$	k_1	117 ± 5	0.808	0.08	1.5×10^{-7}
		Pd^{III} to Pd^{IV}			
$Ni([9]aneN_3)_2^{3+}$	k_2	5700 ± 200	0.075	6000	375
Co_{aq}^{3+}	k_1	770 ± 150	0.990	1×10^{-12}	1050
	k_2	$(3.1 \pm 0.3) \times 10^5$	0.570	5.0	70

[a] Rate constants in M^{-1} s^{-1}. [b] Potentials in V.

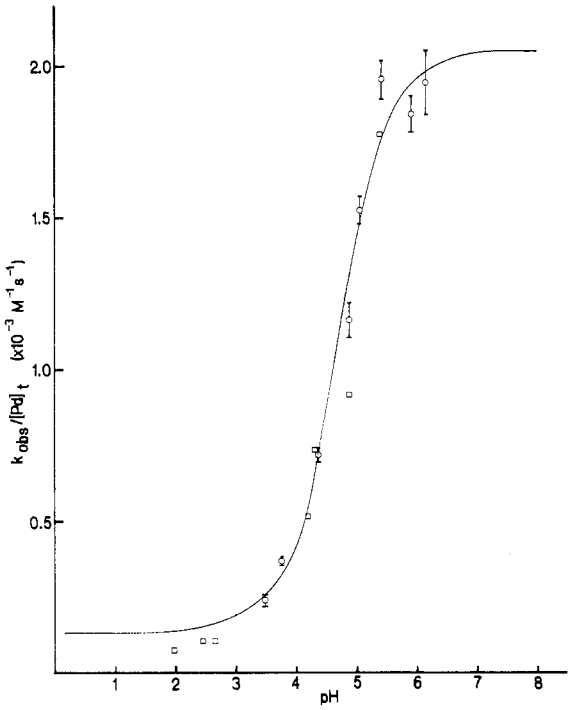

Figure 6. Plot of $k_{obsd}/[Pd(II)]_t$ vs pH for the oxidation by $Ni([9]aneN_3)_2^{3+}$: (○) rate determined from a single Pd(II) concentrations. Only the points determined from several concentrations were employed in the nonlinear least-squares analysis.

are provided as supplementary Tables III(S) and IV(S) and Figure 2(S).

A mechanism consistent with the data may be expressed as

$$Pd^{II}(L)_2^{2+} + Ni(III) \xrightarrow{k_1} Pd^{III}(L)_2^{3+} + Ni(II) \quad (11)$$

$$Pd^{II}(L)(LH)^{3+} + Ni(III) \xrightarrow{k_2} Pd^{III}(L)(LH)^{4+} + Ni(II) \quad (12)$$

$$Pd^{II}(LH)_2^{4+} + Ni(III) \xrightarrow{k_3} Pd^{III}(LH)_2^{5+} + Ni(II) \quad (13)$$

$$Pd^{II}(L)(LH)^{3+} \rightleftharpoons Pd(L)_2^{2+} + H^+ \quad (14)$$

$$Pd^{II}(LH)_2^{4+} \rightleftharpoons Pd^{II}(L)(LH)^{3+} + H^+ \quad (15)$$

where L and LH are the non- and monoprotonated forms of the coordinated ligand. Equations 11–15 lead to the rate expression

$$\text{rate} = \frac{k_1K_aK_{a'} + k_2K_{a'}[H^+] + k_3[H^+]^2}{K_aK_{a'} + K_{a'}[H^+] + [H^+]^2}[Pd(II)]_t[Ni(III)]_t \quad (16)$$

where k_1, k_2, and k_3 are defined above, and the subscript "t" denotes the total concentration of the appropriate reagent. Application of a nonlinear least-squares program to the kinetic data using eq 16 provided the following constants: $k_1 = 2060 \pm 75$ M^{-1} s^{-1}, $k_2 = 120 \pm 100$ M^{-1} s^{-1}, and $k_3 = 50 \pm 50$ M^{-1} s^{-1}, for the oxidation by $Ni([9]aneN_3)_2^{3+}$, with equilibrium constants of $K_a = 2.1 \times 10^{-5}$ M, and $K_{a'} = 4.2 \times 10^{-3}$ M. For the reaction involving $Ni(Me[9]aneN_3)_2^{3+}$, $k_1 = 1800 \pm 70$ M^{-1} s^{-1}, $k_2 = 96 \pm 70$ M^{-1} s^{-1}, and $K_a = 1.7 \times 10^{-5}$ M. The limited pH range used in this study prohibited accurate values of k_3 and $K_{a'}$ from being obtained. Values of $k_3 \approx 30$ M^{-1} s^{-1} and $K_{a'} \approx 4 \times 10^{-3}$ M were compatible with the data. In both analyses, the equilibrium constants were varied independently of the computer program to provide the best fit to the observed rate constants.

The $Pd([9]aneN_3)_2^{2+}$ complex is not an obligatory outer-sphere reductant since the solution geometry is putatively square planar, which leaves the axial sites available for coordination, leading to an inner-sphere electron transfer. However, both of the Ni(III) complexes react via outer-sphere pathways, and the reactions may be treated by the Marcus cross-correlation[31] to obtain an estimate of the electron self-exchange rate for the $Pd^{2+/3+}$ couple. The cross-reaction rate constant, k_{12}, is related to the individual self-exchange rates, k_{11} and k_{22}, and the overall equilibrium constant, K_{12}, by

$$k_{12} = (k_{11}k_{22}K_{12}f_{12})^{1/2}W_{12} \quad (17)$$

$$\ln f_{12} = \frac{[\ln K_{12} + (w_{12} - w_{21})/RT]^2}{4[\ln (k_{11}k_{22}/A_{11}A_{22}) + (w_{11} + w_{22})/RT]} \quad (18)$$

$$W_{12} = \exp[-(w_{12} + w_{21} - w_{11} - w_{22})/2RT] \quad (19)$$

$$A_{ii}/r^2 = [4\pi N\nu_n\delta_r/1000]_{ii} \approx 3 \times 10^{10} \text{ dm}^3 \text{ mol}^{-1} \text{ A}^{-2} \text{ s}^{-1} \quad (20)$$

The work terms, w_{ii}, are derived from the energy necessary to bring the appropriate species to a separation distance, r, in the activated complex. A_{ii} is the diffusion rate for the species ii, r is the sum of the ionic radii, ν_n is the nuclear frequency that destroys the activated complex, and δ_r is the thickness of the reaction layer. N is Avogadro's constant.

For the known self-exchange rates[1c,18] (6×10^3 M^{-1} s^{-1}; 6.1×10^3 M^{-1} s^{-1}) and potentials (0.945 V; 0.955 V) for $Ni([9]aneN_3)_2^{3+/2+}$ and $Ni(Me[9]aneN_3)_2^{3+/2+}$, respectively, and the $Pd^{2+/3+}$ electrode potential ($E_I = 0.398$ V in acetate media), application of the above equations to the Pd(II)–Ni(III) cross-reaction yields values of 3.2×10^{-6} M^{-1} s^{-1} and 1.7×10^{-6} M^{-1} s^{-1} for k_{22}, respectively. This self-exchange rate for the nonprotonated $Pd^{2+/3+}$ couple is extremely low and is indicative of the substantial structural rearrangements necessary for the electron transfer.

The H^+-catalyzed reaction pathway is dominated by the monoprotonated Pd(II) species in this pH range although a value for the diprotonated Pd(II) pathway may be calculated. The lower self-exchange rate constants 7.5×10^{-8} M^{-1} s^{-1} and 3.3×10^{-8} M^{-1} s^{-1} for the $Pd(L)(LH)^{4+/3+}$ couple were calculated by using the E_{IV} potential (0.462 V). This decrease is larger than would be provided by the change in charge (and, hence, work terms) and is therefore indicative of a greater inner-sphere reorganizational energy necessary for electron transfer. Similar analysis of the diprotonated Pd(II) pathway is not informative due to the low precision of the rate constants. Further studies on the oxidation of the Pd(II) species will provide more information on the acid-catalyzed oxidation pathways.

Reduction of $Pd([9]aneN_3)_2^{3+}$. The reduction has been investigated using $Co([9]aneN_3)_2^{2+}$ and $Co(sep)^{2+}$ (sep = 1,3,6,8,10,13,16,19-octaazabicyclo[6.6.6]eicosane) in neutral media ($\mu = 0.2$ M) using both buffered and nonbuffered solutions. The reaction was studied under pseudo-first-order conditions with either the Pd(III) or the Co(II) in >10-fold excess. The disappearance of the Pd(III) absorption was monitored at $\lambda = 370$ and 350 nm

(31) (a) Marcus, R. A. *Annu. Rev. Phys. Chem.* **1964**, *15*, 155; *J. Phys. Chem.* **1963**, *67*, 853. (b) Macartney, D. H.; Sutin, N. *Inorg. Chem.* **1983**, *22*, 3530.

for the two reductants, respectively. Changes in monitoring wavelength had no affect upon the observable rate. The rate constants are included in Table IV.

The pH's of the reactions were maintained above the pK_a value, and consequently, the dominant species is $Pd([9]aneN_3)_2^{3+}$. Slight decreases in the rate were observed at lower pH, which may be due to the participation of some protonated forms of the complex.

With excess Pd(III), the second-order rate constants for the reactions were 560 ± 100 and 117 ± 5 M^{-1} s^{-1} for $Co(sep)^{2+}$ and $Co([9]aneN_3)_2^{2+}$. The Marcus cross-correlation, as outlined above, and the self-exchange rates constants (5.1 M^{-1} s^{-1}; 0.08 M^{-1} s^{-1})[19,20] and potentials (−0.30 V; −0.41 V) for $Co(sep)^{2+/3+}$ and $Co([9]aneN_3)_2^{2+/3+}$, respectively, yielded values of 1.9×10^{-6} M^{-1} s^{-1} and 1.5×10^{-7} M^{-1} s^{-1} for the self-exchange rate constant of the nonprotonated Pd(III) species. This is consistent with the data from the Ni(III) oxidation kinetics, and thus, a value of $(2 \pm 1) \times 10^{-6}$ M^{-1} s^{-1} is assigned for the $Pd^{3+/2+}$ self-exchange rate constant.

Oxidation of $Pd([9]aneN_3)_2^{3+}$. Both $Ni([9]aneN_3)_2^{3+}$ and Co^{3+}_{aq} have been used as oxidants with the Pd(III) species, generating the unstable Pd(IV) complex ($t_{1/2} \approx 1$ h at pH ≈2). Both reactions were conducted under pseudo-first-order conditions in acidic media (pH <1) at μ = 1.0 M, and were monitored at 380 nm for the disappearance of the Pd(III) absorption. The rate constants are included in Table IV.

The reaction of $Pd([9]aneN_3)_2^{3+}$ with $Ni([9]aneN_3)_2^{3+}$ under acidic conditions shows no significant hydrogen ion dependence. The observed rate of 5700 ± 200 M^{-1} s^{-1} may be ascribed to the reaction of the outer-sphere Ni(III) species with the diprotonated Pd(III) complex.

$$Pd^{III}(LH)_2^{5+} + Ni(III) \xrightarrow{k} Pd^{IV}(L)_2^{4+} + Ni(II) + 2H^+ \quad (21)$$

By the use of the self-exchange rate[1c] and redox potential for $Ni([9]aneN_3)_2^{3+}$ together with the redox potential for the $Pd^{III}(LH)_2^{5+}$ species (E_c), a self-exchange rate constant of 375 M^{-1} s^{-1} may be calculated.

The oxidation of $Pd([9]aneN_3)_2^{3+}$ by Co^{3+}_{aq} follows a simple two-term rate law with an inverse hydrogen ion dependence. A mechanism consistent with the data may be expressed as

$$Pd(LH)_2^{5+} + Co^{3+}_{aq} \xrightarrow{k_1} Pd(L)_2^{4+} + Co^{2+}_{aq} + 2H^+ \quad (22)$$

$$Pd(LH)_2^{5+} + Co(OH)^{2+}_{aq} \xrightarrow{k_2} Pd(L)_2^{4+} + Co^{2+}_{aq} + H^+ \quad (23)$$

$$Pd(L)(LH)^{4+} + Co^{3+}_{aq} \xrightarrow{k_3} Pd(L)_2^{4+} + Co^{2+}_{aq} + H^+ \quad (24)$$

Equations 22–24 lead to a rate expression

$$\text{rate} = \frac{k_1[H^+] + k_2K_a + k_3K_b}{[H^+] + K_a + K_b}[Pd(III)]_t[Co(III)]_t \quad (25)$$

where K_a and K_b are the dissociation constants for the Co^{3+}_{aq} and the $Pd^{III}(LH)_2^{5+}$ species, respectively. This expression may be simplified if $[H^+] \gg K_a + K_b$, as is the case, leading to an observed rate constant

$$k_{obsd} = k_1 + [k_2K_a + k_3K_b][H^+]^{-1} \quad (26)$$

It should be noted that since the Pd(IV) complex is octahedral with all the amines coordinated, the oxidation process formally involves the loss of the protons, presumably prior to the electron-transfer step.

The observed kinetics have been analyzed by a nonlinear least-squares program using a modification of eq 26. For k_1, a rate constant of 770 ± 150 M^{-1} s^{-1} was obtained from the intercept while a value of 800 ± 80 M^{-1} s^{-1} was obtained for $k_2K_a + k_3K_b$, from the slope. From the Marcus cross-correlation and the value of k_1, the known redox potentials of the Co^{3+}_{aq} (1.86 V) and diprotonated Pd(III) species (0.870 V), and the self-exchange rate for Co^{3+}_{aq} (1×10^{-12} M^{-1} s^{-1}), a self-exchange rate constant of 1050 M^{-1} s^{-1} is calculated for the $Pd^{3+/4+}$ couple. This is in reasonable agreement with the rate obtained from the $Ni([9]aneN_3)_2^{3+}$ oxidations providing a value of $(7 \pm 3) \times 10^2$ M^{-1} s^{-1} for the self-exchange rate constant for $Pd^{3+/4+}$. This value compares favorably with the observed self-exchange rate of 6×10^3 M^{-1} s^{-1} for the $Ni([9]aneN_3)_2^{3+/2+}$ couple, which involves comparative geometry changes upon oxidation although there is a difference in the overall charge for the ions.

Interpretation of the $k_2K_a + k_3K_b$ term is not simple due to the proton ambiguity that arises from the speciation of the complexes. A reverse application of the Marcus cross-correlation allows a value for k_{12} of a reaction to be calculated. For the reaction between $Co(OH)^{2+}_{aq}$ and $Pd(LH)_2^{5+}$, a rate constant of 1800 M^{-1} s^{-1} is obtained from the $Co(OH)^{2+}_{aq}$ self-exchange rate (5 M^{-1} s^{-1}), potential (1.44 V), and equilibrium constant (2×10^{-3} M) and the $Pd(LH)_2^{5+}$ self-exchange rate determined above. Since this value is larger than the observed value of $k_2K_a + k_3K_b$, it is suggested that the k_3 pathway is only a minor one in contribution to the overall rate. Further investigations into the oxidation of the Pd(III) species are presently being undertaken.

Pd(II)/Pd(IV) Conproportionation. Since the UV–vis spectra of the three oxidation states do not overlap significantly, it is possible to monitor the appearance of the $Pd([9]aneN_3)_2^{3+}$ species from the reaction of Pd(II) with Pd(IV). The reaction involves only the $Pd([9]aneN_3)_2^{n+}$ complexes, and the value obtained from the Marcus cross-correlation directly must be the mean self-exchange rate for the two reactions.

However, the Marcus cross-correlation can be used to determine the k_{12} value from the self-exchange rates and redox potentials. For the reaction of Pd(II) and Pd(IV) with μ = 0.025 M, ionic strength adjusted values of 6×10^{-7} M^{-1} s^{-1} and 22 M^{-1} s^{-1} are calculated for the $Pd^{2+/3+}$ and $Pd^{4+/3+}$ self-exchange rates, respectively. From these values and ΔE = 0.267 V, a rate constant of 0.5 M^{-1} s^{-1} may be calculated for the cross-reaction, which compares favorably with the measured value of 0.7 M^{-1} s^{-1}.

Theoretical Calculation of Exchange Rates. Comparison of the self-exchange rate constants for the $Pd^{3+/2+}$ and $Pd^{4+/3+}$ couples provides dramatic evidence for the influence of inner-sphere reorganization upon the electron-transfer process. The more than 8 orders of magnitude difference in the self-exchange rate constants for these complexes is due predominantly to the rearrangement necessary in going from a square-planar to an octahedral geometry in the first case and an octahedral to an octahedral geometry in the second case. The origin of the electron in both cases is presumably the d_{z^2} orbital, and hence, electronic factors should not influence the rate.

The Marcus–Sutin[31] model provides a method of evaluating the expected self-exchange rate based upon the intrinsic parameters for the reaction, such as the change in bond lengths and the magnitude of the force constants. The self-exchange rate is given by

$$k_{11} = K_0\nu_n\kappa_n\kappa_e \quad (27)$$

where K_0 is the preequilibrium constant, ν_n the effective frequency of the nuclear vibrations, and κ_n and κ_e are the nuclear and electronic factors, respectively. Self-exchange reactions are assumed to be adiabatic and the electronic factor, κ_e, is set to unity. The preequilibrium constant is determined by the work involved ($w(r)$) in bringing the two components together and thus is dependent upon the size and charges of the reactants. It may be obtained from

$$K_0 = (4\pi Nr^2\delta_r/1000)\exp(-w(r)/RT) \quad (28)$$

where the reaction thickness δ_r is typically 0.8 Å and it is assumed that the reaction occurs at distance $r = (a_1 + a_2)$, where a_1 and a_2 are the radii of the reduced and oxidized species. All other symbols have their usual meaning. The Debye–Hückel expression allows the calculation of $w(r)$ from

$$w(r) = (z_1z_2e^2)/D_sr(1 + \beta r\mu^{1/2}) \quad (29)$$

where z_1 and z_2 are the charges on the two reactants, D_s is the static dielectric constant of the medium, μ is the ionic strength, and $\beta = (8\pi Ne^2/(1000D_skT))^{1/2}$.

The nuclear factor contains contributions from both the inner- and outer-sphere (solvent) reorganization energies

$$\kappa_n = \Gamma \exp[-(\Delta G^*_{out} + \Delta G^*_{in})/RT] \quad (30)$$

$$\Delta G^*_{out} = (\Delta e)^2/4(1/2a_1 + 1/2a_2 - 1/r)(1/D_{op} - 1/D_s) \quad (31)$$

$$\Delta G^*_{in} = \tfrac{1}{2}\Sigma f_i[(d^\circ_1 - d^\circ_2)_i/2]^2 \quad (32)$$

where the nuclear tunneling factor, Γ, is defined by

$$\Gamma = [(\sinh (x/2))/x]^{1/2} \times \exp -[(\Delta G^*_{in}/4h\nu_{in})(\tanh (x/4)) - x/4] \quad (33)$$

$$x = h\nu_{in}/kT$$

D_{op} is the optical dielectric constant of the medium, $f_i = 2f_1f_2/(f_1 + f_2)$ is a reduced force constant for the ith inner-sphere vibration, $d^\circ_1 - d^\circ_2 = \Delta d_0$ is the corresponding difference in the equilibrium bond distances in the two oxidation states, and the summation is over all the intramolecular vibrations.

The nuclear frequency term, ν_n, is defined by

$$\nu_n^2 = \frac{\nu_{out}^2\Delta G^*_{out} + \nu_{in}^2\Delta G^*_{in}}{\Delta G^*_{out} + \Delta G^*_{in}} \quad (34)$$

where ν_{out} is given as 0.9×10^{12} s^{-1} ($\nu_{out} = 30$ cm^{-1}) for water and ν_{in} is the reduced metal–ligand stretching frequencies for the complex.

The critical parameter in evaluating these expressions is the determination of the force constants for the metal–nitrogen bonds, which allows the calculation of the inner-sphere reorganization energy. For the Pd(II) complex, the force constant for the bond formed in the axial direction is required. This problem has been solved by considering the fluxional processes involved in the Pd(II) species as determined by variable-temperature NMR.[9] The mechanism involves an interchange mechanism with axial attack of the apical amine. Since this process is the same as half of the inner-sphere reorganization, a value of $2(\Delta G^*_{298})$ or 20.4 kcal/mol is assumed for ΔG^*_{in}.

With $r = 9.0$ Å, $\delta_r = 0.8$ Å, and $\nu_{in} = 470$ cm^{-1} the following parameters are obtained: $K_0 = 0.063$ ($\mu = 0.2$ M), $\Delta G^*_{out} = 5.1$ kcal/mol, and the self-exchange rate is 1×10^{-6} M^{-1} s^{-1}, which is in excellent agreement with the experimental value obtained from the Marcus cross-correlation.

For the $Pd^{4+/3+}$ couple, a reasonable value for the reduced force constant is 275 Nm^{-1} based upon the Pd(IV) force constant[32] and the position of the Pd–N stretching frequencies in the infrared spectrum. With a stretching frequency of 470 cm^{-1} for Pd(III) and 480 cm^{-1} for Pd(IV), a Δd_0 value of 0.12 Å and $r = 9.0$ Å ($\sigma_r = 0.8$ Å), the following parameters are obtained: $K_0 = 0.045$ ($\mu = 1.0$ M), $\Delta G^*_{in} = 8.55$ kcal/mol, and $\Delta G^*_{out} = 5.0$ kcal/mol. A self-exchange rate of 343 M^{-1} s^{-1} is calculated, which is again in excellent agreement with the experimental value.

The agreement between the theoretically calculated and experimentally obtained self-exchange rates suggests that the assumptions made are good approximations of the correct values. For the $Pd^{3+/2+}$ couple it is interesting to reverse the calculation for the inner-sphere reorganization from the value of 20.4 kcal/mol to a value for Δd_0. This involves making two assumptions. The first is that the reduced force constant f_i is not zero but is fairly small (i.e. 10 Nm^{-1}) for the apical metal–nitrogen band and the second is that the bond lengths to the equatorial nitrogens do not alter significantly. The first assumption is based upon recent evidence[29] which suggests that apically positioned nitrogens in a nominally square-planar Pd(II) complex, while not actually bonding to the metal, are interacting sufficiently to distort the square-planar geometry. The second assumption is partially justified by the crystallographic determination[29] of the structure of $Pd(Me[9]aneN_3)_2^{3+}$, which shows very little change in the equatorial bond lengths from those in the $Pd([9]aneN_3)_2^{2+}$ species. A value for Δd_0 of $\approx$1.65 Å may be calculated. From the crystal structure of the Pd(II) cation,[9] the distance between the Pd and the pendant nitrogen is 3.45 Å while the expected bonding distance in the Pd(III) cation should be $\approx$2.1 Å, and thus, $\Delta d_0 \approx 1.35$ Å. The agreement between these two values for Δd_0 suggests that the origin of the large inner-sphere reorganization energy is the coordination of the apical nitrogen to give a six-coordinate precursor and is evidence for the steric role of the ligand in the electron-transfer process.

It is also interesting to note that ready oxidation of the Pd(II) species occurs under mild oxidizing conditions. It is considered that this is facilitated by the fluxional behavior of the Pd(II) complex and the conflict between the steric demands of the ligand and the metal center. Further investigation into the coordination of small macrocycles is proceeding with a view to examining this feature.

Acknowledgment. We thank the NSERC (Canada) and the University of Victoria for their financial support. We are also grateful to Dr. C. Macdonald for his assistance. T.W.W. would like to thank the NSERC for a Post-graduate Scholarship.

Registry No. $[Pd([9]aneN_3)_2](PF_6)_3$, 115512-04-4; $[Pd([9]aneN_3)_2](PF_6)_2$, 114977-77-4; $PdCl_2$, 7647-10-1; $Ni([9]aneN_3)_2^{3+}$, 86709-81-1; $Ni(Me[9]aneN_3)_2^{3+}$, 112816-36-1; $Co([9]aneN_3)_2^{2+}$, 91760-59-7; $Co(sep)^{2+}$, 63218-22-4; $Pd([9]aneN_3)_2^{2+}$, 114977-76-3; $Pd([9]aneN_3)_2^{4+}$, 115512-05-5; $Co([9]aneN_3)_2^{3+}$, 89637-25-2; $Pd([9]aneN_3)_2(ClO_3)_2$, 115512-06-6; $Pd([9]aneN_3)_2Cl_2$, 114977-75-2; $Pd(L)(LH)^{3+}$, 115588-27-7; $Pd(LH)_2^{4+}$, 115588-28-8; $Pd(L)(LH)^{4+}$, 115512-07-7; $Pd(LH)_2^{5+}$, 115588-29-9; $Pd(L)(L\text{-}H)^{3+}$, 115512-08-8.

Supplementary Material Available: Tables I(S) and II(S), containing calculated and observed electrode potentials, Tables III(S) and IV(S), containing rate constants for oxidation of $Pd^{II}([9]aneN_3)_2^{2+}$, Figure 1(S), showing the UV–visible spectra for the Pd(II), Pd(III), and Pd(IV) oxidation states, and Figure 2(S), showing the pH profile of the $Ni^{III}(Me[9]aneN_3)_2^{3+}$ oxidation of $Pd^{II}([9]aneN_3)_2^{2+}$ (8 pages). Ordering information is given on any current masthead page.

(32) Nakamoto, K. *Infrared and Raman Spectra of Inorganic and Coordination Compounds*; Wiley: Toronto, Canada, 1978, and references therein.